Journal of International Scientific Publications:
Materials, Methods & Technologies, Volume 7, Part 2
ISSN 1313-2539, Published at: http://www.scientific-publications.net

NANOSTRUCTURED TIN OXIDE FOR GAS SENSOR APPLICATION

Sergiy M. Malovanyy, Olga I. Milovanova, Edward V. Panov
V.I.Vernadskyi Institute of general & inorganic chemistry, Ukrainian national academy of science –
Palladina ave. 32/34, Kyiv, Ukraine 03680
E-mail: msergii@ukr.net

Abstract

Tin dioxide (SnO_2) is the most important material for use in gas sensing. The performance of SnO_2 sensor is directly related to the tin oxide particle size and compositional characteristics. In the present study, a method for the preparation of pure or chemically modified SnO_2 nano-powders by chemical interaction in molten salts is presented. The molten alkali metal nitrates $NaNO_3$ and KNO_3 were used as liquid reaction medium. The oxides prepared in molten salts consist of small particles (~ 6-10 nm) with narrow size distribution. The particles are united into soft associates with an average size of 200 – 300nm. It was found that SnO_2 nano-powders have good stability against recrystallization process at elevated temperatures up to 650^0C. The sensors were fabricated using thick film technology and tested for ethanol and acetone vapor detection. SnO_2 film exhibits high sensitivity to vapors at a low operating temperature of 200°C. Preliminary results indicate potential application of the material for gas sensors.

Key words: *gas sensors, tin dioxide nanopowder, molten salt synthesis, ethanol and dimethylketone vapors.*

INTRODUCTION

Tin dioxide semiconductor gas sensors were first proposed (Seiyama et al., 1962) in 1962. Since then SnO_2 gas sensors have undergone extensive research and development. Tin dioxide (SnO_2) is the most important material for use in gas sensing. It is the main choice for solid-state gas detectors in domestic, commercial and industrial application due to the low operating temperatures, high sensitivities, simplicity of sensor design and low manufacturing costs (Ihokura et al., 1994; Yamazoe 1992; Jimenez et al., 1996).

Ethanol and dimethylketone vapors are the most exhaustively studied gases in the field of gas sensing due to the great demand in biomedical, chemical, and food industries, especially in wine-quality monitoring and traffic safety (Tang et al., 2007). Although ethanol and acetone have similar sensor response the discrimination between these two vapors is essential for the precise and reliable screening of intoxicated drivers. The expiration from a diabetes patient can contain a small amount of acetone vapor (Ryabsev et al., 1999), therefore, a sick diabetes patient might be mistaken for a drunk driver. Biomedical and traffic safety applications require ethanol and/or dimethylketone vapor sensing at the presence of other reducing vapors, thus requires high selectivity for certain compound.

New methods such as non-invasive diagnostics by human breath analysis bear the potential to drastically reduce the costs of medical care (Cao et al., 2006). Standard medical diagnostics has reached the limit of further economization as trained human resources are required. Some of the endogenous compounds found in human breath, such as dimethylketone, ethanol, ammonia, ethane and pentane, have been successfully identified as breath markers for several diseases (Manolis 1983).

Dimethylketone is a specific breath marker for type-1 diabetes and its concentration increases from 300 to 900 ppb for healthy humans and to more than 1800 ppb (Deng et al., 2004) for diabetic patients. Currently, breath acetone testing is carried out using gas chromatography followed by flame ionization detection (Sanchez and Sacks 2003), ion mobility spectrometry (Lord et al., 2002) and MS detection (Phillips et al., 1999). These methods need bulky instrumentation and skilled operator. So, these methods are not very suitable for use in diabetes diagnostics and dimethylketone monitoring outside the laboratory. To meet the requirements for clinic applications, the sensing devices also need, in addition to sensitivity and selectivity, sufficient portability and reasonable production cost. That is why, tin dioxide semiconductor gas sensors, which have a strong miniaturization while offering very high sensitivities down to ppb range, may become a key technology for commercial implementation of breath analysis.

Because of an increasing demand for fast, continuous, and trace detection, current research in gas sensor techniques has been focused on the development of sensors which can provide low-cost, portable, rapid sensory, and high sensing information. A general route to improve a sensor's characteristics is to make the chemical sensors at the nanoscale, taking advantage of large surface areas of nanoscale structures (Kwon et al., 1999; Comini 2006; Xue et al., 2005) and to change compositional characteristics (i.e. the presence of additives) (Gopel and Schierbaum 1995; Xu et al., 1991). For instance, tin dioxide sensor performance (stability, sensitivity, selectivity, and response time) has been improved considerably by reducing the size of the particles used in the sensors to nanometer dimensions (Krius et al., 1998; Zang and Liu 2000) and/or by adding dopants (noble metals or other metal oxides) to tin dioxide to create nanocomposite materials (Siciliano 2000; Cabot et al., 2000).

This study aims at preparing gas-sensing nanocomposites on the basis of doped SnO_2 using chemical interaction in molten salt synthesis method and testing their sensing properties for detection of ethanol and dimethylketone vapors.

EXPERIMENTAL

The nanocrystalline powders of pure tin dioxide or doped SnO_2 were prepared by molten salts interaction method (Andriiko et al., 2004). A tin(II) chloride dihydrate was used as the main precursor for SnO_2 synthesis. The metal salts (doping additives) of antimony chloride, iron (III) chloride, nickel chloride, bismuth chloride or lead chloride were dissolved in molten $SnCl_2$ at 40^{o}C for a total doping cation to tin cation ratio varying from 0,005 to 0,05. Prepared solid solutions of chlorides were finally ground into powder. In order to synthesize nano-particles, powders of the solid solution of chlorides were added by portions to molten alkali metal nitrates (pure KNO_3 or $NaNO_3$ - KNO_3 eutectic mixture) under agitation. Reaction mixture was kept at 420^{o}C for 1h. The interaction in the molten nitrates resulted in the formation of oxides as follows:

$$SnCl_2 + 2KNO_3 \rightarrow SnO_2 + 2KCl + 2NO_2\uparrow$$

The melt was cooled down to room temperature and washed six to seven times with distilled water to remove water soluble salts (nitrates and chlorides) and dried at 120^{o}C.

The nanocomposite of noble metal (Pt, Pd) particles and tin dioxide-based nanopowder were prepared by controlled reductive precipitation of metal particles onto agglomerates of doped SnO_2 crystallites in a water solution. A diluted solution of hexachloroplatinic acid and/or palladium dichloride was added to an aqueous suspension of tin dioxide-based nanopowder under agitation. Final dropwise addition of water solutions of sodium formate and sodium ascorbate to the suspension resulted in the reduction of noble metal cations to metal particles. Following precipitation, the powder was aged for 24h, and then

separated by decantation, washed several times with distilled water to remove the sodium cations and dried at 120°C for 2h.

The as-prepared powder was mixed with organic solvent terpineol for slurry preparation. After ultrasonic treatment the paste was painted onto insulating alumina substrate. The applied film was dried at 150°C for 2h and then annealed at 500°C for 2h in the atmosphere of inert gas argon. The sensor response to ethanol and dimethylketone vapours was examined using a two-channel gas calibration system with a computerized picoammeter unit. The operation temperature was varied between 100 and 400°C.

RESULTS AND DISCUSSION

Powder X-ray diffraction (XRD) data was collected on a Dron-4 powder diffractometer using Cu Kα radiation (λ = 1.5405 Å) operating from 2θ = 10-80°. The phase analysis of prepared samples showed that in the as-prepared state and after annealing, the SnO_2 – based powders display, regardless of chemical composition, only cassiterite phase lines, and there is no evidence of the presence of any other oxide phase.

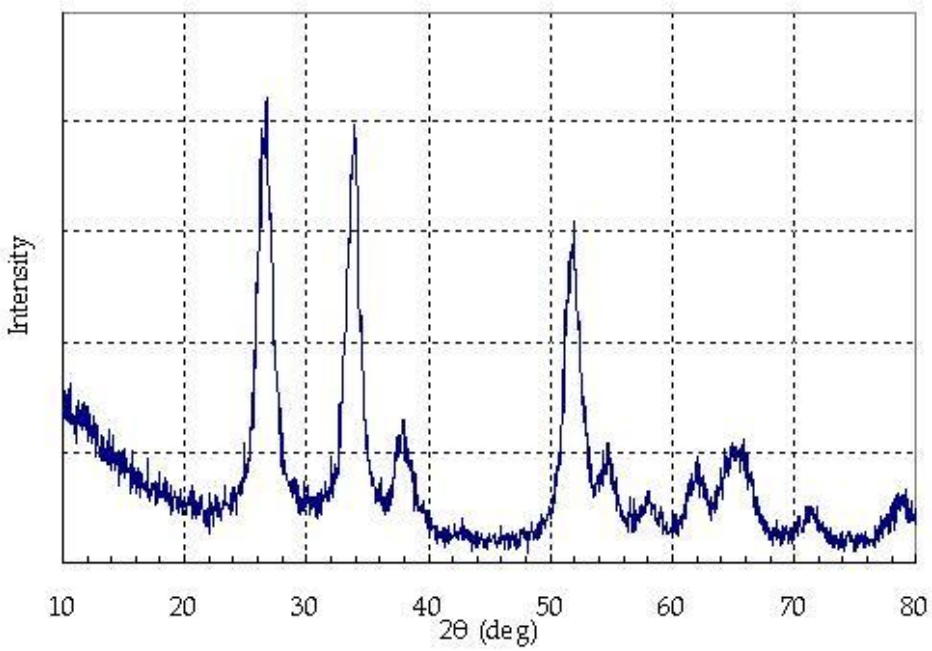


Fig.1. XRD pattern of pure SnO_2 prepared via molten salt synthesis procedure at 420°C.

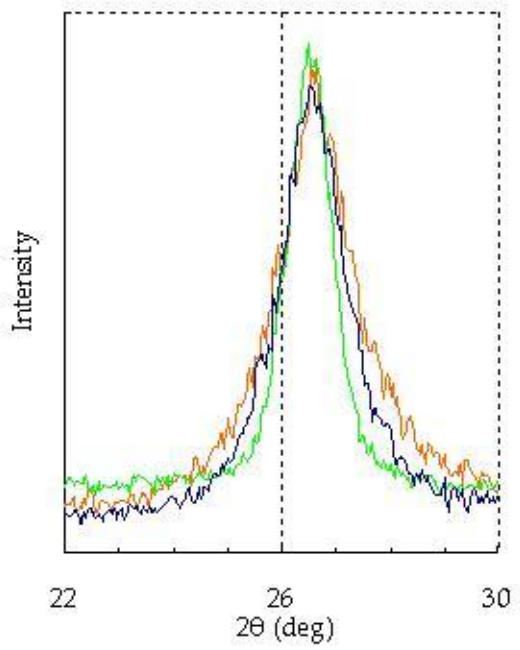


Fig.2. XRD patterns of SnO_2-PbO, 110 reflection. PbO content: 1.5 mol% - green; 3.0 mol% - blue; 6.0 mol% - orange lines.

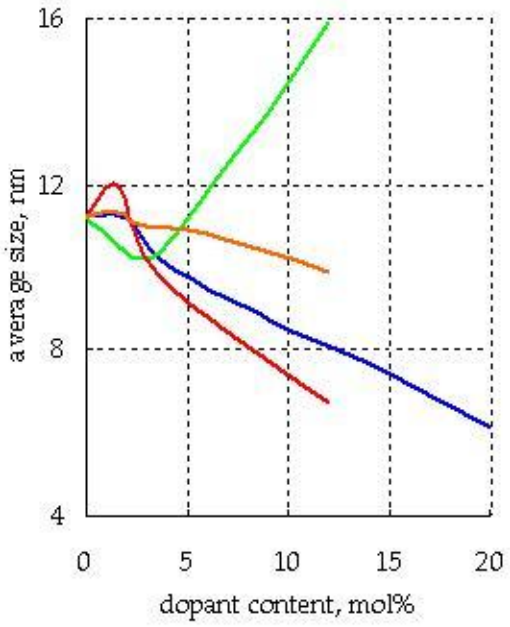


Fig.3. Correlation between crystallite size of SnO_2-MeO and dopant content. MeO : NiO – green; PbO – red; $BiO_{1.5}$ – blue; $SbO_{1.5}$ – orange lines.

Figure1 shows that all lines of XRD pattern are greatly broadened, which indicates that the chemical interaction in the molten alkali nitrates results in the formation of tin dioxide-based nanopowder. The crystallite size, d, was calculated from the X-ray line width using the Scherrer formula, $d = 0.9\lambda/\beta_{1/2}\cos\theta$, where λ is the X-ray wavelength, $\beta_{1/2}$ is the width of the diffraction peak at half-height, and θ is the diffraction angle. For crystallite size estimation, the broadening of three main diffraction peaks of SnO_2 at $2\theta = 26.5^o$, 33.7^o and 52.0^o has been studied in order to rule out the possible influence of other factors, besides crystallite size, on line width. As is shown in Fig. 2 and Fig.3, the d value depends largely on the dopant content and depends on the chemical nature of the dopants. It was found that all tested dopants can be divided into three groups according to their influence on the crystallite size of SnO_2 nanopowder (Fig.3.). The d value decreases with dopant content in the case of the use of lead oxide (PbO) or bismuth oxide (Bi_2O_3). The use of nickel (NiO) or copper (CuO) oxides for tin dioxide additive indicated an opposite effect of crystallite size increase. To the third group of oxide dopants we referred additives, which had no clear effect on the d value like antimony and niobium oxides.

The morphologies of tin dioxide powders were studied using a TEM (JEM2100F, JEOL) equipped with EDX (Oxford Instruments) for elemental analysis. Fig. 4 shows TEM images of SnO_2 samples. There is a good correlation between the average crystallite size calculated on the basis of an analysis of X-ray maximum profile and actual dimensions of particles obtained by TEM. It is obvious that the samples with dopants have less agglomeration and are distributed more uniformly than the pure sample (Fig.5). This demonstrates that the metal oxide dopants inhibit the aggregation of particles during high temperature interaction in molten salts reaction medium, during melt separation and final thermal treatment of the powder. Elemental analysis of tin dioxide sample surface modified by noble

metals (Pt and Pd) did not prove uniform distribution of metal clusters, but indicated that metal particles are smaller than doped SnO_2 crystallites and thus cannot be clearly visually indentified from TEM images (Fig.6, Table 1).

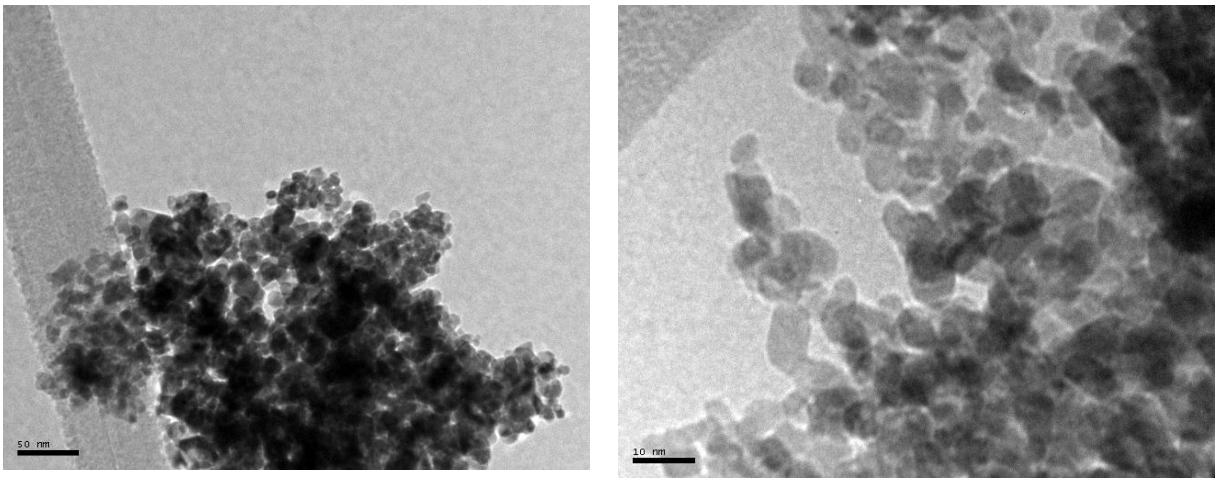


Fig.4. TEM images of undoped SnO_2 with different magnification.

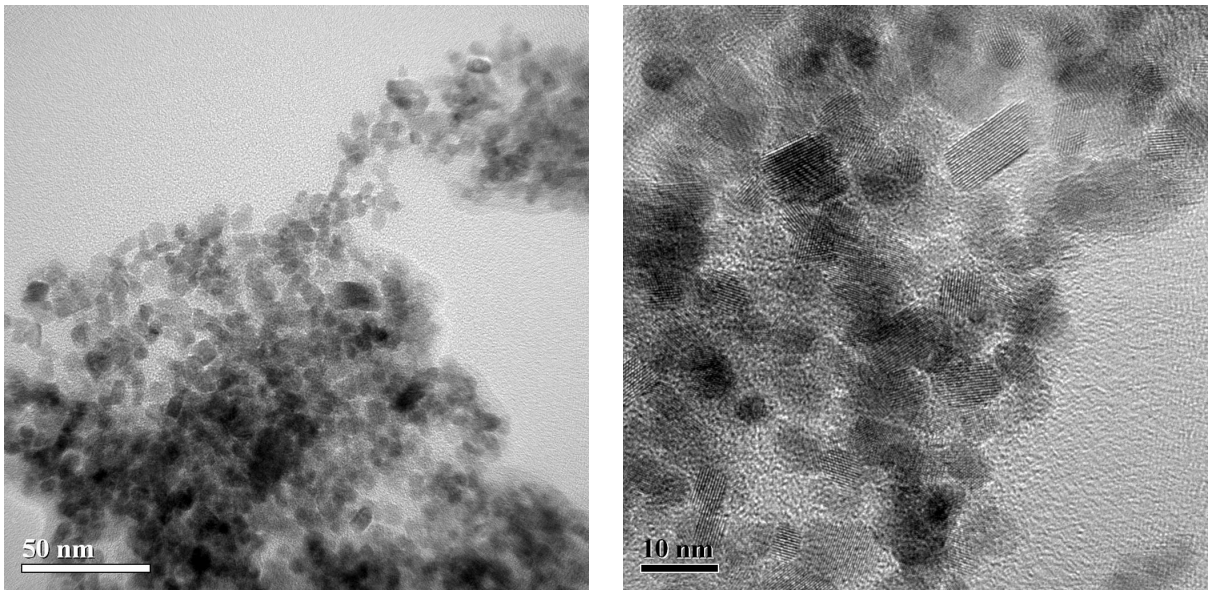


Fig.5. TEM images of Sb-doped SnO_2. $SbO_{1.5}$ content is 3 mol%.

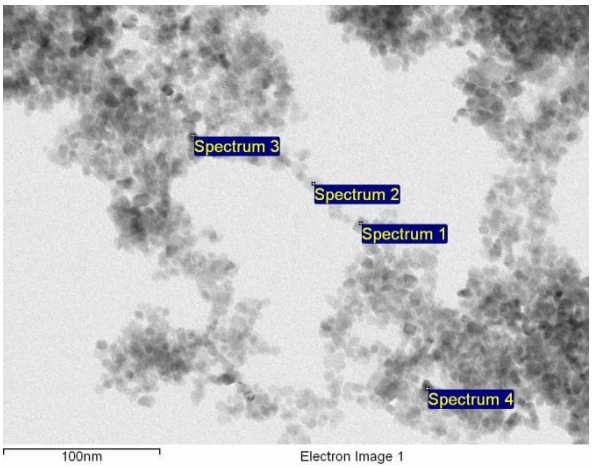


Fig.6. TEM images of SnO_2-$SbO_{1.5}$/Pd/Pt. with selected points for EDX analysis. Additives contents: Sb - 3 mol%; Pd - 3wt%; Pt -1wt%.

	O	Sn	Pd	Pt
Spectrum 1	68.63	31.37	-	-
Spectrum 2	69.09	27.97	2.81	0.14
Spectrum 3	61.87	27.80	8.41	1.86
Spectrum 4	54.22	26.32	16.18	2.65

Table 1. Elemental analysis results for selected points (Fig.6). All results in atomic %.

Operating temperature had an effect on the gas sensitivity and selectivity. The tin dioxide-based nanocomposites were sensitive to ethanol and dimethylketone at temperatures between 100°C and 400°C. The optimal operating temperature to ensure high selectivity to distinguish ethanol and acetone and retain fairly high sensitivity is 200°C. Sensitivity and selectivity to ethanol and dimethylketone vapors of SnO_2-based materials were examined under different conditions to see the effects of oxide composition and vapor concentration on the sensitivity. Fig.7 shows the results of response to ethanol at 200°C on tin dioxide doped by antimony oxide (Sn to Sb ratio is 32), which was surface modified by metallic particles of noble metals (Pt and Pd). The nanocomposite had the highest sensitivity among tested compositions. The detectable concentration limit of ethanol vapor is below 500ppb, which is acceptable for most breath analysis applications. The antimony-doped SnO_2 without noble metal catalysts at the same test conditions demonstrated much lower sensitivity of 1.2 even at high ethanol vapor concentration of 300ppm. A similar sensor behavior was observed in the presence of dimethylketone vapor (Fig.8). $Sn_{0.97}Sb_{0.03}O_2$ material exhibits relatively poor sensitivity of 1.1 to 300ppm of acetone at 200°C. The sensitivity changed dramatically for the sample modified by platinum (1 wt. %) and palladium (3 wt. %) and reached the value of 3.8 for 10ppm of dimethylketone. The enhanced gas sensitivity could be attributed to small grain size of the oxide and to the presence of catalyst (noble metal) nanoparticles.

One can see (Fig.9) that SnO_2-based film has a typical relationship between sensitivity and vapor concentration. Both for dimethylketone and for ethanol sensitivity increases with vapor content and reaches the value of 8.5 for 100ppm demethylketone concentration and 22.0 for 100ppm of ethanol.

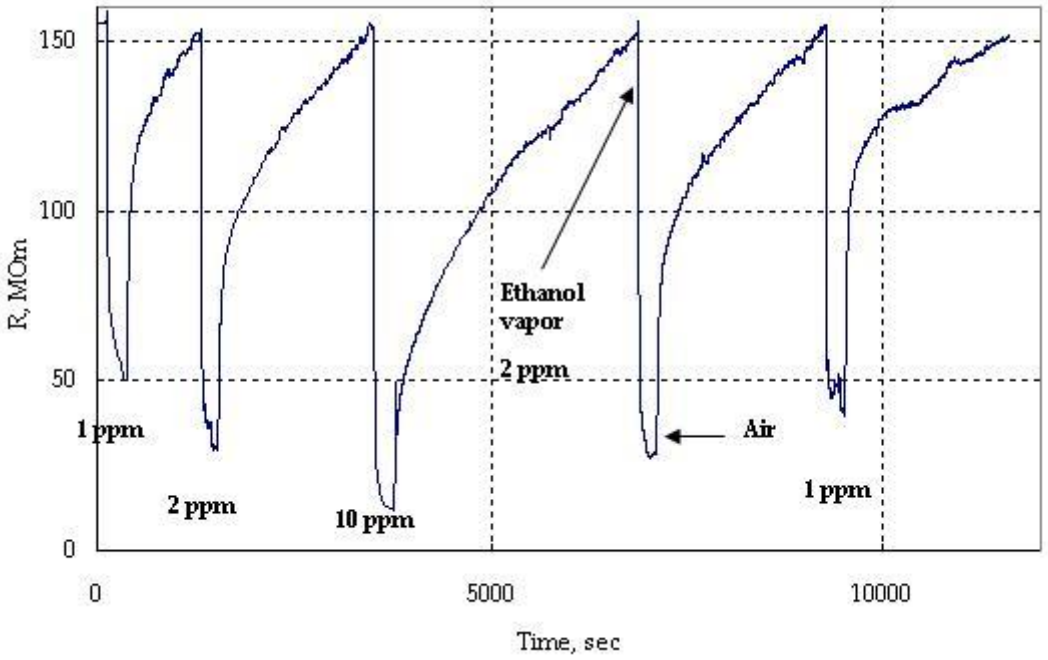


Fig.7. Response and recovery of SnO_2-$SbO_{1.5}$/Pd/Pt sensor to different concentration of ethanol vapor at 200°C.

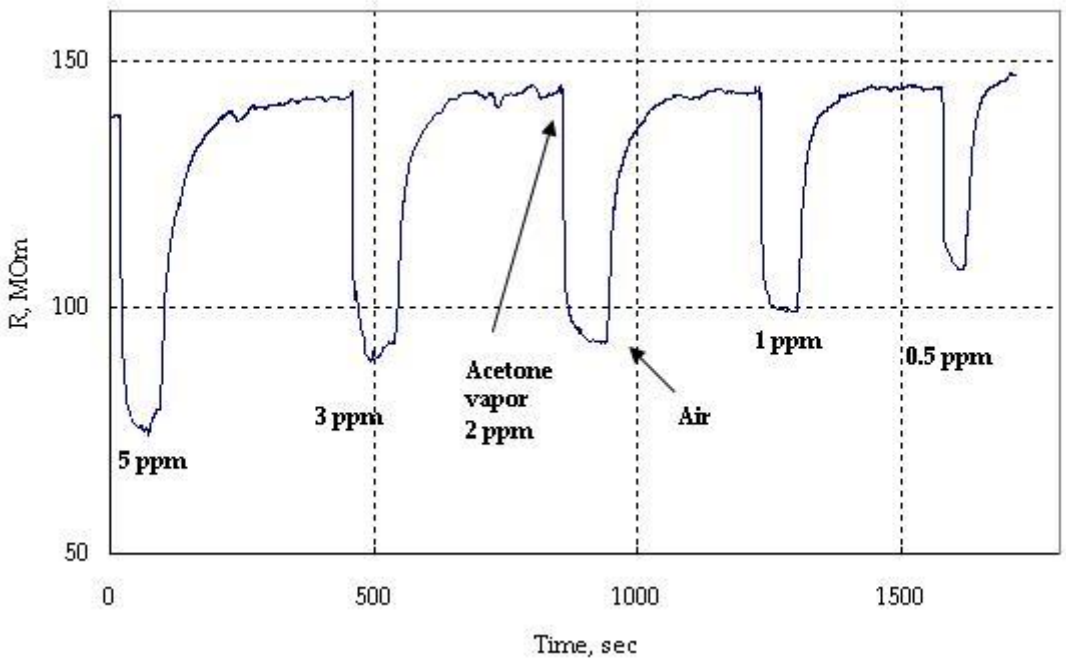


Fig.8. Response and recovery of SnO_2-$SbO_{1.5}$/Pd/Pt sensor to different concentration of dimethylketone vapor at 200°C.

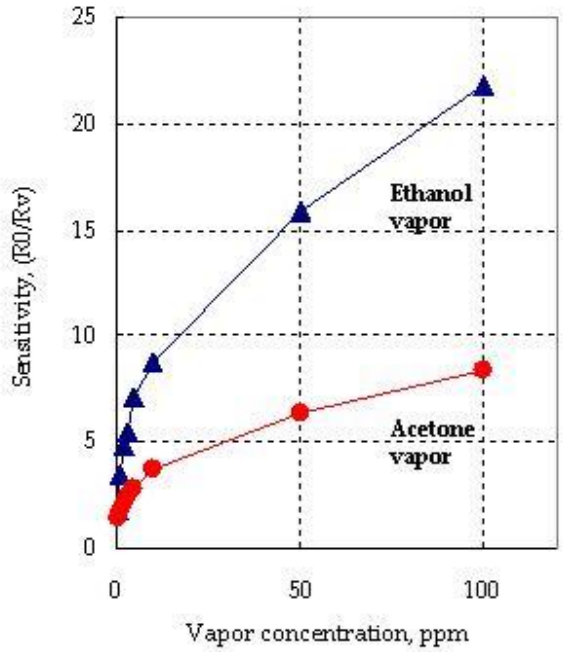


Fig.9. Sensitivity of SnO_2-$SbO_{1.5}$/Pd/Pt sensor to different concentration of dimethylketone and ethanol vapors at 200°C.

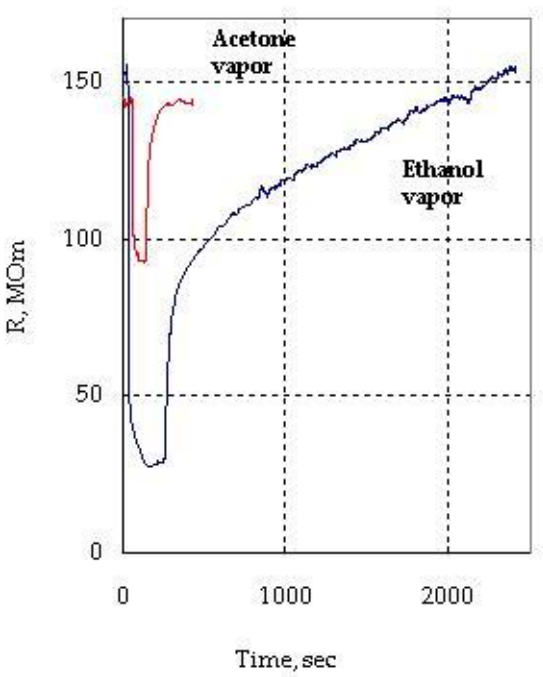


Fig.10. Response and recovery of SnO_2-$SbO_{1.5}$/Pd/Pt sensor to 2ppm concentration of ethanol and dimethylketone vapor at 200°C.

Generally, the response to ethanol is similar to that to acetone due to their similar chemical nature. Indeed, many papers (Gong et al., 1999; Li et al., 2002) reported that oxide semiconductor-type gas sensors show similar sensing behavior towards ethanol and acetone regardless of the sensing materials. According to test data (Fig.10), SnO_2 – based nanocomposite thick film responses to ethanol and dimethylketone vapor have main difference in the desorption zone. Desorption process for dimethylketone is fast, and film signal relaxation is complete in 150 seconds after gas supply stop. The same process for ethanol vapor is much slower and lasts up to 1800 seconds. This effect of different desorption kinetics on low-temperature (200°C) thick film is a basis for discrimination between ethanol and dimethylketone in gas mixtures. Fig.10 shows that sensor response 150 seconds after its contact with vapor mixture may be attributed only to response to ethanol.

CONCLUSIONS

The nanopowders for SnO_2 – based thick film sensors with various compositions were prepared by molten salt synthesis method. The composites of tin dioxide with noble metals showed good response to low concentrations (below 1ppm) of both ethanol and dimethylketone vapors at relatively low temperatures of 200°C. Although the sensing behavior of ethanol and acetone is similar, successful discrimination between them can be realized by the analysis of desorption process, which is much slower for ethanol.

REFERENCES

1. A.A. Andriiko, A A. Furman, S.M. Malovanyy, U.S. Patent 6787231 (2004).

2. A. Cabot, J. Arbiol, J.R. Morante, U. Weimar, N. Barsan, W. Gopel, Sens. Actuators B 70, 87 (2000).

3. W.Q. Cao and Y.X. Duan, Clin. Chem. 52, 800 (2006).

4. E. Comini, Anal. Chim. Acta. 568, 28 (2006).

5. C.H. Deng, J. Zang, X.F. Yu and X.M. Zang, J. Chromatogr. B810, 269 (2004).

6. H. Gong, Y.J. Wang, S.C. Teo, L. Huang, Sens. Actuators B 54, 232 (1999).

7. W. Gopel and K.D. Schierbaum, Sens. Actuators B 26, 1 (1995).

8. K. Ihokura, J. Watson, The Stannic Oxide Gas Sensor – Principles and Applications. CRC Press, Boca Raton, FL, 1994.

9. V.M. Jimenez, A.R. Gonzalez-Elipe, J.P. Espinos, A. Justo, A. Fernandez, Sens. Actuators B 31, 29 (1996).

10. F.E. Krius, H. Fissan, A. Peled, J. Aerosol. Sci. 29, 511 (1998).

11. T.H. Kwon, J.Y. Ryu, W.C. Choi, S.W. Kim, S.H. Park and M.K. Lee, Sens. Mater. 11, 257 (1999).

12. X. Li, G. Zang, F. Cheng, B.Guo, J. Electrochem. Soc. 153, H133 (2006).

13. H. Lord, Y.F. Yu, A. Segal abd J. Pawliszyn, Anal. Chem. 74, 5650 (2002).

14. A. Manolis, Clin. Chem. 29, 5 (1983).

15. M. Phillips, J. Herrera, S. Krishnan, M. Zain, J. Greenberg, R. Cataneo, J.Chromatogr. B 729, 75 (1999).

16. S.V. Ryabsev, A.V. Shaposhnick, A.N. Lukin, E.P. Domashevskaya, Sens. Actuators B 59, 26 (1999).

17. J.M. Sanchez and R.D. Sacks, Anal. Chem. 75, 2231 (2003).

18. T. Seiyama, A. Kato, K. Fujiishi, M. Nagatani, Anal. Chem. 34, 1502 (1962).

19. P. Siciliano, Sens. Actuators B 70, 153 (2000).

20. H. Tang, Y. Li, C. Zheng, J. Ye, X. Hou, Talanta 72, 1593 (2007).

21. C. Xu, J. Tamaki, N. Miura, N. Yamazoe, Sens. Actuators B 3, 147 (1991).

22. X.Y. Xue, Y.J. Chen, Y.G. Wang and T.H. Wang, Appl. Phys. Lett. 86, 233101 (2005).

23. N. Yamazoe, Sens. Actuators B 6, 9 (1992).

24. G. Zang, M. Liu, Sens. Actuators B 69, 144 (2000).